

Holistically discretise the Swift-Hohenberg equation on a scale larger than its spatial pattern

A. J. Roberts*

November 13, 2018

Abstract

I introduce an innovative methodology for deriving numerical models of systems of partial differential equations which exhibit the evolution of spatial patterns. The new approach directly produces a discretisation for the evolution of the pattern amplitude, has the rigorous support of centre manifold theory at finite grid size h , and naturally incorporates physical boundaries. The results presented here for the Swift-Hohenberg equation suggest the approach will form a powerful method in computationally exploring pattern selection in general. With the aid of computer algebra, the techniques may be applied to a wide variety of equations to derive numerical models that accurately and stably capture the dynamics including the influence of possibly forced boundaries.

Keywords: pattern evolution, finite element discretisation, Swift-Hohenberg equation, centre manifold theory.

PACS: 02.60.Lj, 02.70.Dh, 02.30.Oz

Contents

1 Introduction

2

*Department of Mathematics and Computing, University of Southern Queensland, Toowoomba, Queensland 4352, AUSTRALIA. <mailto:aroberts@usq.edu.au>

1	<i>Introduction</i>	2
2	Develop a centre manifold discretisation	3
3	Boundary conditions are straightforwardly determined	6
4	Conclusion	10
	References	10

1 Introduction

The evolution of spatial patterns is an important area of research. One example of interest itself and serving as a model for other systems is Rayleigh-Bénard convection [19, 10, 13, e.g.] in which a fluid layer is heated from below and cooled from above. The flow flow self organises into an evolving pattern of upwelling and downwelling. One of the most useful models describing such pattern evolution, for example see [5, (9)], [13, (2.11)] or [11, (13)], is the Ginzburg-Landau equation which we consider in in one spatial dimension:

$$a_t = ra + ca_{xx} - d|a|^2a \quad (1)$$

where $a(x, t)$ is the (complex) amplitude of the pattern in any locale, subscripts denote partial derivatives, and r , c and d are specific constants. The Ginzburg-Landau equation describes the evolution of the complex amplitude of spatially periodic structures as they evolve and interact. The derivation of the Ginzburg-Landau equation in any specific pattern problem is fundamentally based upon the underlying structure varying slowly in space-time. However, here in §2 we derive the discrete form

$$\dot{a}_j = ra_j + \frac{c}{h^2}(a_{j+1} - 2a_j + a_{j-1}) - d|a_j|^2a_j \quad (2)$$

of the Ginzburg-Landau equation (1) without ever invoking slow space-time variations. Following earlier research introducing holistic discretisation [17], the derivation is rigorously based upon centre manifold theory [2, 3, e.g.] and ensures the discretisation faithfully models the underlying system.

One amazing consequence of this approach is that we straightforwardly incorporate physical boundaries into the discrete model. Boundaries have significant effects on the pattern evolution [19, 6, e.g.]. Previously there have only been limited, usually just linear [5, p937–8, e.g.], arguments about how to incorporate such boundaries into the analysis to give boundary conditions

for the Ginzburg-Landau equation (1). But here we use nonlinear analyses to derive appropriately modified modifications of (2) near the boundary to account for its effects. In §3 we discuss time dependent Dirichlet and Neumann boundaries as two examples. Our approach resolves the subgrid fields within each element. Near a boundary the method resolves the modifications to the subgrid fields due to the influence of the boundary and thus naturally creates a discretisation appropriate to the specified boundary condition.

As a simple prototype pattern evolution problem, we here consider the Swift-Hohenberg equation [21] in one spatial dimension:

$$u_t = ru - (1 + \partial_x^2)^2 u - u^3. \quad (3)$$

This equation has often been used, as we do here, to investigate issues in pattern selection [7, 8, e.g.], especially the influence of physical boundaries in 2D [10, 1, e.g.]. Linearly, the Swift-Hohenberg equation (3) has spatially periodic solutions $u \propto \exp(\lambda t + ikx)$ for wavenumber k where the growth-rate

$$\lambda = r - (1 - k^2)^2. \quad (4)$$

Thus for parameter $r < 0$ all spatial modes decay, whereas for $r > 0$ a band of modes near $|k| = 1$ may grow. Exactly at the critical parameter $r = 0$, all modes decay except for the two neutral modes $\exp(\pm ix)$. We construct a holistic numerical discretisation based upon these neutral modes.

2 Develop a centre manifold discretisation

Here we develop a model of the system using invariant manifold theory. The analysis is essentially local in space, it resolves structures over a number of “convective rolls”. Previous use of invariant manifold theory [9] has generally sought global models evolving on the so-called inertial manifold [22, e.g.].

Exactly at criticality, long lasting solutions are 2π -periodic in x . As shown schematically in Figure 1, introduce artificial internal boundaries every p periods, spacing $h = p2\pi$. These divide the domain into elements, each centred on a grid point x_j . Denote the field in the j th element by $u_j(x, t)$. The internal boundary conditions (IBCs) to hold at each end of an element are chosen to be the nonlocal conditions

$$u_j + \frac{\partial u_j}{\partial x} = (1 - \gamma) \left[u_j + \frac{\partial u_j}{\partial x} \right]_{x=x_j-h/2}$$

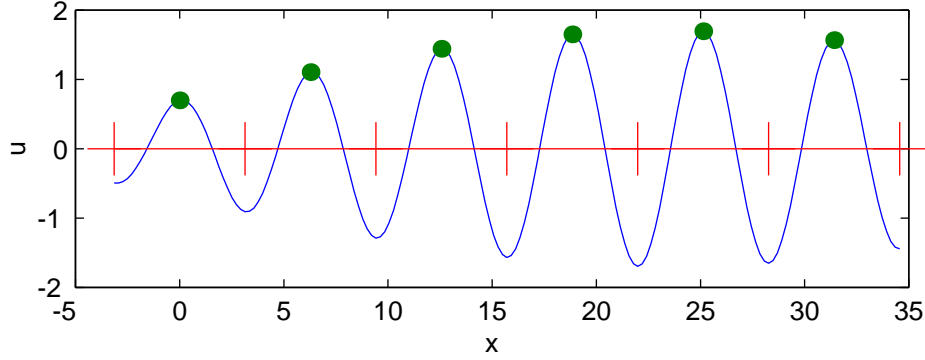


Figure 1: schematics diagram showing a varying “roll” structure (solid curve) discretised by introducing artificial internal boundaries every period ($p = 1$) at odd multiples of π (vertical bars). The “roll” field in the j th element is parametrised by the amplitude a_j (discs).

$$+ \gamma \left(u_{j+1} + \frac{\partial u_{j+1}}{\partial x} \right) \quad \text{at } x = x_j + h/2, \quad (5)$$

$$u_j - \frac{\partial u_j}{\partial x} = (1 - \gamma) \left[u_j - \frac{\partial u_j}{\partial x} \right]_{x=x_j+h/2} + \gamma \left(u_{j-1} - \frac{\partial u_{j-1}}{\partial x} \right) \quad \text{at } x = x_j - h/2, \quad (6)$$

and the same for the second derivative $v = u_{xx}$. These IBCs are parametrised by γ which controls the interaction and information flow between adjacent elements. When this coupling parameter $\gamma = 0$ these IBCs reduce to conditions,

$$\left[u_j \pm \frac{\partial u_j}{\partial x} \right]_{x_j-h/2} = \left[u_j \pm \frac{\partial u_j}{\partial x} \right]_{x_j+h/2}, \quad (7)$$

requiring the solution in the j th element is h -periodic—the field and its derivatives at the right end of the element must match smoothly the field at the left end. Whereas when $\gamma = 1$ these IBCs require continuity of the field and its derivatives between abutting ends of adjacent elements,

$$u_j \pm \frac{\partial u_j}{\partial x} = u_{j+1} \pm \frac{\partial u_{j+1}}{\partial x} \quad \text{at } x = x_j + h/2.$$

Thus when the coupling parameter $\gamma = 0$ each element is isolated from all others, whereas when $\gamma = 1$ we ensure enough continuity between elements to recover the Swift-Hohenberg equation (3) throughout the domain. We use

these IBCs to model the Swift-Hohenberg equation, when $\gamma = 1$, by basing analysis on the discrete elements that are isolated at $\gamma = 0$.

Apply centre manifold theory based upon the linear dynamics in uncoupled elements. By notionally adjoining the dynamically trivial equations $\dot{\gamma} = \dot{r} = 0$ we treat all terms with a factor of the coupling parameter γ or the forcing parameter r as “nonlinear” perturbations. h -periodic solutions of the linearised Swift-Hohenberg equation, $u_t = -(1 + \partial_x^2)^2 u$, then are $\exp(\lambda_n t + i k_n x)$ for any integer n with wavenumber $k_n = 2\pi n/h = n/p$ and growth-rate $\lambda_n = -(1 - k_n^2)^2$. Thus within each element all modes decay exponentially except the two modes with wavenumber $k_{\pm p} = \pm 1$ which are neutral. Hence “linearly,” the solution in each element evolves exponentially quickly in time to the roll solution

$$u_j = a_j e^{ix} + b_j e^{-ix}, \quad (8)$$

where a_j and b_j are the complex amplitudes of the rolls—the solution is real if and only if all b_j are the complex conjugate of a_j . Theory [2, 3, e.g.] then assures us that for the original nonlinear Swift-Hohenberg equation, coupled between elements by the IBCs (5–6), there exists a centre manifold \mathcal{M} on which solutions are parametrised by the collection of evolving amplitudes \mathbf{a} and \mathbf{b} :

$$u = u_j(\mathbf{a}, \mathbf{b}, \gamma, r, x) \quad (9)$$

$$\text{such that } \dot{a}_j = g_j(\mathbf{a}, \mathbf{b}, \gamma, r) \quad \text{and} \quad \dot{b}_j = \bar{g}_j(\mathbf{a}, \mathbf{b}, \gamma, r). \quad (10)$$

Moreover, theory assures us quite generally that solutions of the Swift-Hohenberg equation exponentially quickly approach solutions of (10). Lastly, theory asserts that the functions in (9–10) are determined by substitution into the Swift-Hohenberg equation and the internal boundary conditions and then solving to some order in the parameters.

Computer algebra available from the author performs the tedious calculations using an iterative algorithm [15]. However, before undertaking the modelling we define the amplitudes precisely as the element averages

$$a_j(t) = \frac{1}{h} \int_{x_j-h/2}^{x_j+h/2} u(x, t) e^{-ix} dx \quad \text{and} \quad b_j(t) = \frac{1}{h} \int_{x_j-h/2}^{x_j+h/2} u(x, t) e^{+ix} dx. \quad (11)$$

Then the solution field is found to be

$$\begin{aligned} u_j = & a_j e^{+ix} + \frac{\gamma}{4h} e^{+ix} \left[(\delta^2 a_j - 2i\mu\delta b_j) + (4\mu\delta a_j - 2i\delta^2 b_j) x \right] \\ & + b_j e^{-ix} + \frac{\gamma}{4h} e^{-ix} \left[(\delta^2 b_j + 2i\mu\delta a_j) + (4\mu\delta b_j + 2i\delta^2 a_j) x \right] \\ & + \mathcal{O}(\gamma^3 + A^3 + r^{3/2}), \end{aligned} \quad (12)$$

where $A = \|\mathbf{a}\| + \|\mathbf{b}\|$ measures the overall amplitude of the solution field¹ and where μ and δ are central mean and difference operators, $\mu a_j = (a_{j+1/2} + a_{j-1/2})/2$ and $\delta a_j = a_{j+1/2} - a_{j-1/2}$ respectively. These $\mathcal{O}(\gamma)$ terms show the leading order effect of neighbouring elements upon the subgrid field in each element; however, there is as yet no effect upon the evolution which is still neutral $g_j = \bar{g}_j = \mathcal{O}(\gamma^2)$. Using computer algebra to compute the next order of interactions and I find the evolution

$$\dot{a}_j = ra_j + \frac{4\gamma^2}{h^2}\delta^2 a_j - 3\gamma^2 a_j^2 b_j + \mathcal{O}(\gamma^4 + A^4 + r^2), \quad (13)$$

$$\dot{b}_j = rb_j + \frac{4\gamma^2}{h^2}\delta^2 b_j - 3\gamma^2 a_j b_j^2 + \mathcal{O}(\gamma^4 + A^4 + r^2). \quad (14)$$

Evaluating these at the coupling parameter $\gamma = 1$ we recover a numerical model for the Swift-Hohenberg equation which is just the discrete version (2) of the appropriate Ginzburg-Landau equation (1).

In this approach there is little merit in discussing equivalent PDEs to the derived discrete models (13–14). The reason is that here the element size h must contain an integral number of rolls and so the limit $h \rightarrow 0$ is not physically valid. For the same reason, there appears to be no merit in seeking consistency with a PDE as done for other holistic discretisations [18]. In this approach we should discuss the numerical model as it stands. But it is relevant to observe that the long-wave limit, slow variations in j , should and does reduce to the relevant Ginzburg-Landau equation (1).

3 **Boundary conditions are straightforwardly determined**

Now consider the boundaries to the physical domain. For simplicity suppose that the conditions at the boundary, say the left boundary, are either one of the two cases:

$$u = (-1)^p \alpha(t) \quad \text{and} \quad u_{xx} = (-1)^p \beta(t); \quad (15)$$

$$\text{or} \quad u_x = (-1)^p \alpha(t) \quad \text{and} \quad u_{xxx} = (-1)^p \beta(t). \quad (16)$$

These physical boundary conditions are incorporated into the analysis by replacing the left-hand IBC (6) of the left-most element, say element $j = 1$, by a boundary condition corresponding to one of (15) or (16). Consequently this

¹A multinomial term $\gamma^l A^m r^n$ is $\mathcal{O}(\gamma^q + A^q + r^{q/2})$ if and only if $l + m + 2n \geq q$.

left physical boundary is, without loss of generality, located at $x = x_1 - h/2$. However, we want this left-most element, $j = 1$, to still have the neutral periodic solution (8) when the inter-element coupling parameter $\gamma = 0$. Thus we actually replace the left-hand IBC (6) of the left-most element by

$$u_1 - \frac{\partial u_1}{\partial x} = (1 - \gamma) \left[u_1 - \frac{\partial u_1}{\partial x} \right]_{x=x_1+h/2} \mp \gamma \left(u_1 + \frac{\partial u_1}{\partial x} \right) \pm 2(-1)^p \gamma \alpha(t) \quad \text{at } x = x_1 - h/2, \quad (17)$$

and similarly for $v = u_{xx}$. When the coupling parameter $\gamma = 0$ (17) reduces to requiring h -periodic solutions. Whereas when $\gamma = 1$ (17) reduces to

$$(1 \pm 1)u_1 - (1 \mp 1) \frac{\partial u_1}{\partial x} = \pm 2(-1)^p \alpha \quad \text{at } x = x_1 - h/2,$$

and similarly for $v = u_{xx}$, which for the upper choice of signs specifies the even derivative BC (15) and for the lower choice of signs specifies the odd derivative BC (16). Other specific boundary conditions may be treated similarly, but here I just restrict attention to these two cases.

Computer algebra constructs the centre manifold model for both alternative boundary conditions: (15) giving the upper alternative of plus/minus signs seen below; and (16) giving the lower alternative. The leading order influence of the boundary forcing upon the field in the leftmost element is

$$\begin{aligned} u_1 = & e^{ix} a_1 + \frac{\gamma}{4h} e^{ix} [(-2 \pm i)a_1 + a_2 \mp b_1 - ib_2] \\ & + 2(\pm ia_1 + a_2 \pm (1 \pm 2i)b_1 - ib_2)x] \\ & \pm \frac{\gamma^2 \alpha}{h} e^{ix} \left[\frac{7 + 5i}{16} - \frac{2 + 3i}{4}x + \frac{1 - i}{96}(h^2 - 12x^2) \right] \\ & \pm \frac{\gamma^2 \beta}{h} e^{ix} \left[\frac{3 + i}{16} - \frac{i}{4}x + \frac{1 - i}{96}(h^2 - 12x^2) \right] \\ & + e^{-ix} b_1 + \frac{\gamma}{4h} e^{-ix} [(\mp a_1 + ia_2 - (2 \mp i)b_1 + b_2) \\ & + 2(\pm(1 \mp 2i)a_1 + ia_2 \mp ib_1 + b_2)x] \\ & \pm \frac{\gamma^2 \alpha}{h} e^{-ix} \left[\frac{7 - 5i}{16} - \frac{2 - 3i}{4}x + \frac{1 + i}{96}(h^2 - 12x^2) \right] \\ & \pm \frac{\gamma^2 \beta}{h} e^{-ix} \left[\frac{3 - i}{16} + \frac{i}{4}x + \frac{1 + i}{96}(h^2 - 12x^2) \right] \\ & + \mathcal{O}(\gamma^3 + A^3 + r^{3/2}, |\dot{\alpha}| + |\dot{\beta}|) \end{aligned} \quad (18)$$

See there are two sorts of effects of the boundary: first, the subgrid field

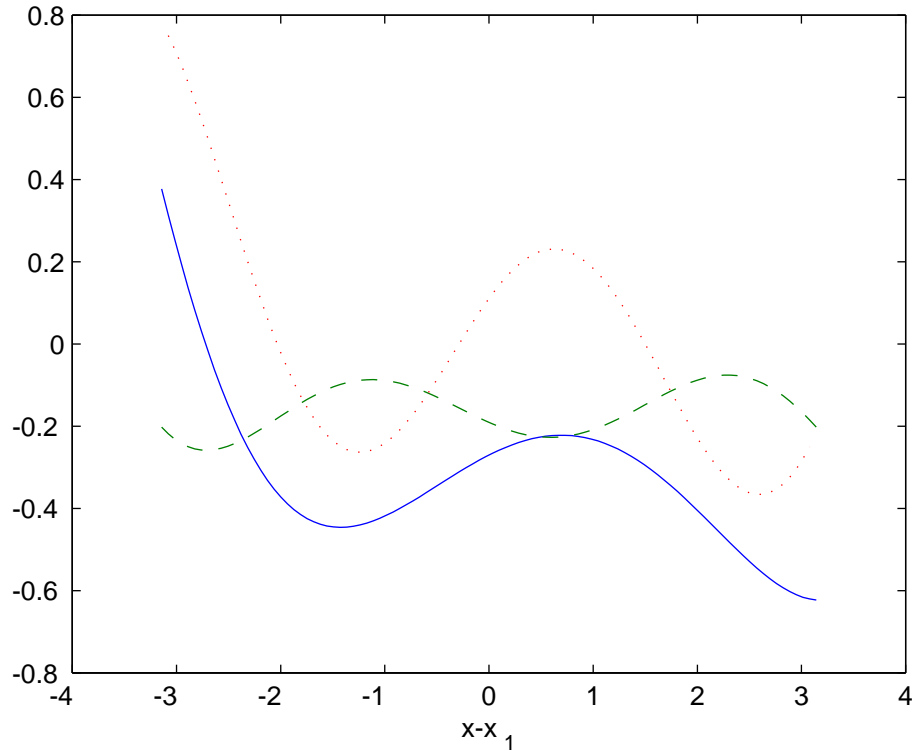


Figure 2: spatial subgrid structure (18) of the coefficients of α (solid), β (dashed) and its second derivative (dotted) when the boundary condition at $x = x_1 - \pi$ is (15) for an element size $h = 2\pi$. These give the field if all amplitudes $a_j = b_j = 0$. See the α and the second derivative curves are at the boundary $x = 0$ about a value of one higher than the field in the bulk of the element—this is appropriate as α specifies the boundary value and β the second derivative.

generated by the grid values of the leftmost two elements differs from that in an interior element (12); secondly, the forcing parametrised by α and β also adjusts the subgrid field. For example, in Figure 2 is plotted the basis of the field in the leftmost element when all grid values $a_j = b_j = 0$. See that they resolve a boundary layer structure on a scale of $\Delta x \approx 1$ —the resolution is crude because this is only the first approximation to the adjustment necessary to account for the boundary. By resolving the subgrid spatial structure near a boundary we will generate appropriate discretisations for the given boundary condition. The resolution of structure near the boundary is important for deriving correct boundary conditions for models [5, p937, e.g.]. As demonstrated in Figure 2, our approach does some of the near boundary

analysis identified in [14] as necessary for deriving boundary conditions for mathematical models such as the differential Ginzburg-Landau equation.

The relevant evolution is obtained by analysing to quadratic terms in the coupling parameter γ . We find that \dot{a}_2 and \dot{b}_2 are identical to that obtained for the interior, (13–14) with $j = 2$. However, the evolution for the amplitude of the rolls in the leftmost element adjacent to the boundary is

$$\begin{aligned} \dot{a}_1 &= ra_1 + \frac{4\gamma^2}{h^2}(a_2 - 2a_1 \mp b_1) - 3a_1^2 b_1 \mp \frac{\gamma^2}{h}(1 - i)(\alpha + \beta) \\ &\quad + \mathcal{O}(\gamma^4 + A^4 + r^2, |\ddot{\alpha}| + |\ddot{\beta}|), \end{aligned} \quad (19)$$

$$\begin{aligned} \dot{b}_1 &= rb_1 + \frac{4\gamma^2}{h^2}(b_2 - 2b_1 \mp a_1) - 3a_1 b_1^2 \mp \frac{\gamma^2}{h}(1 + i)(\alpha + \beta) \\ &\quad + \mathcal{O}(\gamma^4 + A^4 + r^2, |\ddot{\alpha}| + |\ddot{\beta}|). \end{aligned} \quad (20)$$

Set the inter-element coupling parameter $\gamma = 1$ to recover a discretisation. In the absence of boundary forcing, $\alpha = \beta = 0$, we analyse a little of the dynamics near the boundary by supposing for illustrative purposes that $a_1 = a_2 = a$ and $b_1 = b_2 = \bar{a}$ (for real solutions). The evolution equations (19–20) then reduce to

$$\dot{a} \approx ra - \frac{4}{h^2}(a \pm \bar{a}) - 3|a|^2 a. \quad (21)$$

First, consider the upper alternative when u and u_{xx} are specified at the boundary, (15). Linearly, the real part of a will decay at a rapid rate, a negative growth-rate of $r - 8/h^2$; whereas the imaginary part has a growth-rate r . Thus the amplitudes near the boundary will rapidly evolve to be pure imaginary. This corresponds to solutions $u \propto \sin(x)$ as expected for the given boundary conditions. Secondly, consider the converse lower alternative when u_x and u_{xxx} are specified at the boundary, (16). Linearly, the imaginary part of a will decay at a rapid rate, a negative growth-rate of $r - 8/h^2$; whereas the real part has a growth-rate r . Thus the amplitudes near the boundary will rapidly evolve to be purely real. This corresponds to solutions $u \propto \cos(x)$ as expected for the given boundary conditions. Thus the near boundary discretisation (19–20) selects for fields u with evenly spaced rolls located so that u is zero at the boundary in the case of specified even derivatives, and so that the derivatives of u are zero at the boundary in the case of specified odd derivatives. These properties agree with earlier more specific work [19, e.g.]

The presence of boundary forcing will push the system away from its otherwise natural equilibria. For example, for the upper alternative, (21) breaks the symmetry in $\Im(a)$ and predicts an equilibrium $\Re(a) \approx -h(\alpha + \beta)/8$ instead of zero and so there is a change in amplitude and phase of the rolls

near the boundary. Observe that time variations in the forcing, $\dot{\alpha}$ and $\dot{\beta}$, are not significant at this level of approximation: this absence is surprising given the appearance of time derivatives of forcing in other boundary discretisations at finite grid size [16]; the absence is linked to the definition (11) of the amplitudes because other amplitude definitions generate $\dot{\alpha}$ and $\dot{\beta}$ terms in the model. Cox and Roberts [4] showed that special parametrisations could eliminate time dependence upon forcing in a centre manifold—evidently the amplitude definition (11) at least approximates such a parametrisation. The important point is that our treatment of near boundary elements generates discretisations which naturally incorporate the forced boundary conditions.

4 Conclusion

We have introduced a rigorously based method for deriving discrete amplitude equations for the evolution of spatial patterns directly from the original PDEs. The method has been applied to the Swift-Hohenberg equation but the principles apply to a wide variety of PDEs governing spatio-temporal evolution. One remarkable advantage of this direct derivation is that we may also derive appropriate discretisations near any forced boundary.

The generalisation to patterns in 2D space appears a straightforward generalisation of that employed for reaction-diffusion equations [12]. Space would be tessellated in some regular manner by introducing appropriately periodic IBCs. Then a centre manifold model would be constructed with a finite number of basis wavevectors in each element analogous to the regular analysis of Skeldon *et al* [20].

Computer algebra readily determines models of higher-order in the asymptotic expansions, higher-order in both or either of nonlinearity or of stencil width. However, the IBCs (5–6) used then here appear to break a symmetry of the Swift-Hohenberg equation. More research is needed into a better form of the IBCs as well as further applications of the methodology.

Acknowledgement: this research is partially supported by a grant from the Australian Research Council.

References

- [1] M. Bestehorn, R. Friedrich, and H. Haken. Travelling waves in nonequilibrium systems. *Physica D*, 37:295–299, 1989.

- [2] J. Carr. *Applications of centre manifold theory*, volume 35 of *Applied Math. Sci.* Springer-Verlag, 1981.
- [3] J. Carr and R. G. Muncaster. The application of centre manifold theory to amplitude expansions. II. Infinite dimensional problems. *J. Diff. Eqns*, 50:280–288, 1983.
- [4] S. M. Cox and A. J. Roberts. Centre manifolds of forced dynamical systems. *J. Austral. Math. Soc. B*, 32:401–436, 1991.
- [5] M. C. Cross. Boundary conditions on the envelope function of convective rolls close to onset. *Phys Fluids*, 25:936–941, 1982.
- [6] M. C. Cross, P. G. Daniels, P. C. Hohenberg, and E. D. Siggia. Phase winding solutions in a finite container above the convective threshold. *J. Fluid Mech*, 127:155–183, 1983.
- [7] M. C. Cross and A. C. Newell. Convection patterns in large aspect ratio systems. *Physica D*, 10:299–328, 1984.
- [8] M. C. Cross, G. Tesauro, and H. S. Greenside. Wavenumber selection and persistent dynamics in models of convection. *Physica D*, 23:12–18, 1986.
- [9] M. D. Graham, P. H. Steen, and E. S. Titi. Computational efficiency and approximate inertial manifolds for a Bénard convection system. *J. Non-linear Sci.*, 3:153–167, 1993.
- [10] H. S. Greenside and W. M. Coughran. Nonlinear pattern-formation near the onset of rayleigh-benard convection. *Phys Rev A*, 30:398–428, 1984.
- [11] L. Kramer and W. Pesch. Convection instabilities in nematic liquid crystals. *Annu Rev Fluid Mech*, 27:515–541, 1995.
- [12] T. MacKenzie and A. J. Roberts. The dynamics of reaction diffusion equations lead to a holistic discretisation. In R. L. May, G. F. Fitz-Gerald, and I. H. Grundy, editors, *EMAC 2000 Proceedings. Proceedings of the fourth biennial Engineering Mathematics and Applications Conference*, pages 199–202, 2000.
- [13] A. C. Newell, T. Passot, and J. Lega. Order parameter equations for patterns. *Annu. Rev. Fluid Mech.*, 25:399–453, 1993.
- [14] A. J. Roberts. Boundary conditions for approximate differential equations. *J. Austral. Math. Soc. B*, 34:54–80, 1992.

- [15] A. J. Roberts. Low-dimensional modelling of dynamics via computer algebra. *Comput. Phys. Comm.*, 100:215–230, 1997.
- [16] A. J. Roberts. Derive boundary conditions for holistic discretisations of burgers' equation. Technical report, [<http://arXiv.org/abs/math.NA/0106224>], 2001.
- [17] A. J. Roberts. Holistic discretisation ensures fidelity to Burgers' equation. *Applied Numerical Modelling*, 37:371–396, 2001.
- [18] A. J. Roberts. A holistic finite difference approach models linear dynamics consistently. *Mathematics of Computation*, to appear, 2001.
- [19] L. A. Segel. Distant side walls cause slow amplitude modulation of cellular convection. *J. Fluid Mech*, 38:203–224, 1969.
- [20] A. C. Skeldon and M. Silber. New stability results for patterns in a model of long-wavelength convection. *Physica D*, 122:117–133, 1998.
- [21] J. Swift and P. C. Hohenberg. Hydrodynamic fluctuations at the convective instability. *Phys. Rev. A*, 15:319–328, 1977.
- [22] R. Temam. Inertial manifolds. *Mathematical Intelligencer*, 12:68–74, 1990.